processes

MDPI

Article

The Optimized Roadway Layouts and Surrounding Rock Control Technology of the Fully Mechanized Mining Surface with Large Mining Heights in High-Gas Mines

Qi Ma, Yidong Zhang *, Zexin Li, Yu Zheng, Guangyuan Song and Lei Hu

School of Mines, State Key Laboratory of Coal Resources and Safe Mining, China University of Mining and Technology, Xuzhou 221116, China

* Correspondence: ydzhang@cumt.edu.cn; Tel.: +86-13952118118

Abstract: Many problems exist in the layout of working surfaces in high-gas mines, such as the low efficiency of roadway excavation, difficulties in maintenance after excavation, and serious resource wastes due to difficulties in recovering coal pillars between roadways. Taking the project profile in the west wing mining area of Sihe Coal Mine as the background, this work proposed an optimization plan for the staggered-layer arrangement of roadways. The minimum retained size of the coal pillar was calculated through theoretical analysis, and the plastic failure and deformations of surrounding rocks under different coal pillar sizes and roadway layouts were compared based on finite difference numerical simulations. The reasonable retained size of the coal pillar was determined to be 45 m, and the roadway layout was determined according to the distribution of coal and rock strata in the mining field. The technical measures of base angle pressure relief blasting and strengthening support were proposed to ensure the safety and stability of surrounding rocks of roadways during the service period after the layout plan was optimized. Similar simulation tests were used to study the damage deformations and stress changes of the blasting pressure relief floor. On-site tests showed that the optimized roadway layout greatly improved the recovery rate of coal resources. In addition, surrounding rocks had good stability, and they could be simply repaired or serve the next working surface directly without being repaired. These research results provide a scientific basis and useful reference for similar projects.

Keywords: high-gas mine; large-scale mining; optimization of roadway layouts; pressure relief blasting; surrounding rock control

Citation: Ma, Q.; Zhang, Y.; Li, Z.; Zheng, Y.; Song, G.; Hu, L. The Optimized Roadway Layouts and Surrounding Rock Control Technology of the Fully Mechanized Mining Surface with Large Mining Heights in High-Gas Mines. *Processes* **2022**, *10*, 2657. https://doi.org/10.3390/pr10122657

Academic Editor: Yong Yuan

Received: 10 October 2022
Accepted: 7 December 2022
Published: 9 December 2022

1. Introduction

Coal resources as China's main energy source have remained unchanged for a long time, according to the characteristics of China's energy storage status for resources such as oils, gases, and coal [1,2]. Moreover, coal resources are not affected by the international situation, which guarantees China's industrial construction and economic development. The annual output of coal resources will reach 6 billion tons in the middle of the 21st century in terms of the current situation of industrial construction and economic development. Affected by coal resources, the coal mining method is mainly underground mining. Mine disasters from water, fires, gases, coal dust, and roof accidents are encountered during the mining process (see Figure 1). A total of 750 large gas accidents occurred in 12 years from 2005 to 2016, which accounts for 53.6% of all accidents. In addition, roof accidents also account for a large proportion [3,4]. Mining affects roadways, especially for large-scale mining with high working surfaces, and the stability of surrounding rocks cannot be guaranteed.

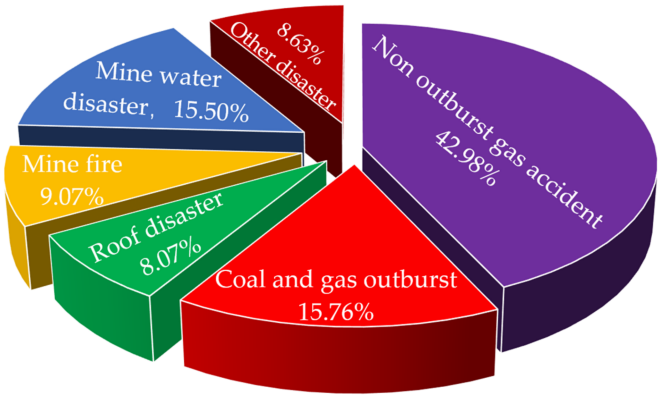

Figure 1. Mine accident distribution [5].

When coal resources are recovered from thick coal and high-gas mines, more multi-lane arrangements are used to prevent gas disasters and ensure the air volume of the working surface. A certain width of coal pillars between each roadway should be retained to ensure the stability of the surrounding rocks of roadways, which results in great resource waste. Therefore, mines should optimize the roadway layout of the fully mechanized mining surface with the large mining height in high-gas mines and put forward the corresponding surrounding rock control technology.

Researchers have studied the optimized layout of the working surface roadway. Zhang et al. [6,7] combined the coal seam occurrence of the Lu'an mining area to optimize the layout of comprehensive coal mining roadways for high-gas thick coal seams. High alley pumping with Y-shaped ventilation or gob-side entry retaining with W-shaped ventilation and high alley pumping are adopted for the gob-side entry retaining of the fully mechanized mining surface. Technical measures for reinforcement along the empty lane have been proposed to ensure the safe and efficient mining of high-gas comprehensive discharge surfaces. Zhang et al. [8–12] used various research methods to analyze the stress distribution law of residual coal pillar floor during mining of close-range coal seams, the stability of coal pillars in sections, the deformations and failure of surrounding rocks in roadways, the internal energy accumulation of coal pillars in sections, and the failure caused by coal rock masses of floor. The coal pillar sizes and alternate distance of mining roadways during the down-going combined mining of shallow coal seams were studied to optimize mining roadway layouts in close-range coal seams. This provided the resource recovery rate and ensured the stable use of mining roadways during the service period.

Bai et al. [13–15] used the mechanical model of key block B under the small coal pillar in the limit equilibrium method. Key block B does not slip and rotate unsteadily in this case. Numerical simulation software was used to analyze stress in the mining field when roadways were arranged along the coal seam roof and floor at different coal pillar widths. Compared with the wide coal pillar, the narrow one has a considerable stabilizing effect on coal pillar roadways, which is more conducive to the conservation and recovery of coal resources. Sun [16–18] proposed an optimization plan for roadway layouts based on gas prevention and control, production costs, and continuity during mining under the multi-roadway layout of the high-gas fully mechanized mining surface. Gas prevention and control effects and economic benefits are significant after the comprehensive roadway layout is optimized.

Kang [19–21] summarizes the main achievements in the surrounding rock control of roadways in coal mines since the establishment of New China. The control technology is divided into five categories: surface support, anchoring, modification, pressure relief, and joint control. Kang [19–21] also analyzes the existing problems in surrounding rock control in coal mine roadways. Zhang et al. [22–25] believe that the combined action of the bolt group causes bolts and rock masses within their anchoring range to form a bearing structure with certain strength based on the stress of the roadway bolt (cable) after support.

This structure plays a vital role in roadway stability and is called an anchoring composite supporting body. The influence of the bolt density on the bearing characteristics of the anchoring supporting body is systematically studied, which provides a novel theoretical basis for controlling the surrounding rocks of roadways.

Cheng et al. [26–28] studied the blasting pressure relief mechanism to solve the on-site problem that the deep high-stress heaving floor of soft rock roadways restricts the safe and efficient mining of coal mines. Joint control technology for grouting the reinforced heaving floor was proposed based on pressure relief blasting. Loosening blasting technology was used to block the high-stress propagation path and release pressures on floor. The control effect of surrounding rocks of roadways is obvious after using the technical scheme. Zuo et al. [29,30] established an equivalent elliptical model of pressure relief grooving in view of the large variability and difficulties in the support of deep soft rock roadways. The change law of the surrounding stress field before and after grooving the circular roadway was analyzed by Mohammad [31–36] to reveal the stability control mechanism of surrounding rocks for pressure relief grooving.

Zhu et al. [37–39] aimed at the technical characteristics such as the obvious sinking of the roof of the deep large-section roadway, the violent convergence of the two sides, and strong floor heaving. The stability of surrounding rocks of roadways was ensured by the multi-level staggered dense high-strength bolt (cable) support technology, multi-layer concrete spraying arch support, and anchor net injection of a grouting reinforcement arch behind the wall and pillar–wall poured concrete reinforcement.

Researchers have studied the optimized roadway layouts and surrounding rock control technology instead of optimized roadway layouts under the complex ventilation system of high-gas mines. Combined with the production profile of the W2302 working surface of Shanxi Sihe Coal Mine, this work used on-site research, theoretical analysis, numerical simulations, and on-site actual measurement methods to optimize the roadway layout and reduce the coal pillar size. Corresponding technical measures for surrounding rock control were proposed to reduce the repair rate of roadways, which improved the coal resource recovery rate and achieved safe and efficient production.

2. Engineering Application Overview

Coal $3^{\#}$ was mined in the west wing mining area of Sihe Coal Mine, with an average thickness of 6.08 m, an average burial depth of 402.29 m, and an average inclination angle of the coal seam of 4°. According to the measurement results of the absolute gas gushing quantity, the mine had high gas content in the W2302 working surface. The production of the working surface adopted a three-intake two-return ventilation method and one-time full-height comprehensive mechanized mining to control and prevent gas disasters and ensure ventilation.

The W2303 working surface was located on the north side of the W2302 working surface (see Figure 2). When the 2302 working surface was mined, there were inlet airways 1, 2, and 3 and return airways 1 and 2 (hereinafter referred to as I_1, I_2, I_3, V_1, and V_2, respectively) from north to south. A 35 m coal pillar was retained between I_3 and V_1, and a 20 m coal pillar was retained between V_1 and V_2 to ensure the stability of the surrounding rocks of roadways.

Fresh air entered from I_1, I_2, and I_3, and ventilation air was discharged from V_1 and V_2 during mining of the working surface. The W2303 face was mined again after mining the W2302 face was stopped. V_1 and V_2 of the W2302 working surface were repaired and used as I_1 and I_2 of the W2303 working surface. The arrangement had the following disadvantages, which were not conducive to the safe and efficient mining of coal resources. First, 55 m wide coal pillars were left between the two working surfaces, which resulted in a great waste of non-renewable resources. Second, gas discharge needed to be carried out in advance during excavating roadways to ensure safe excavation, and the excavation efficiency was low. Meanwhile, mining roadways were laid under coal seams, and the stability of surrounding rocks was not easy to control during the service period of roadways.

It was intended to optimize the roadway layout of the working face with high gas and high mining heights and propose the corresponding stability control measures of surrounding rocks. The optimized roadway layout is shown in Figure 3.

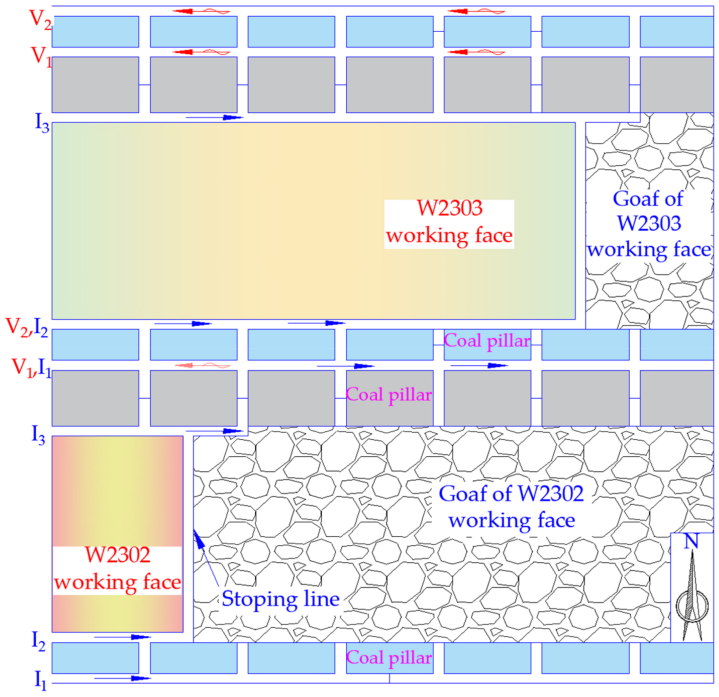

Figure 2. Mining layout.

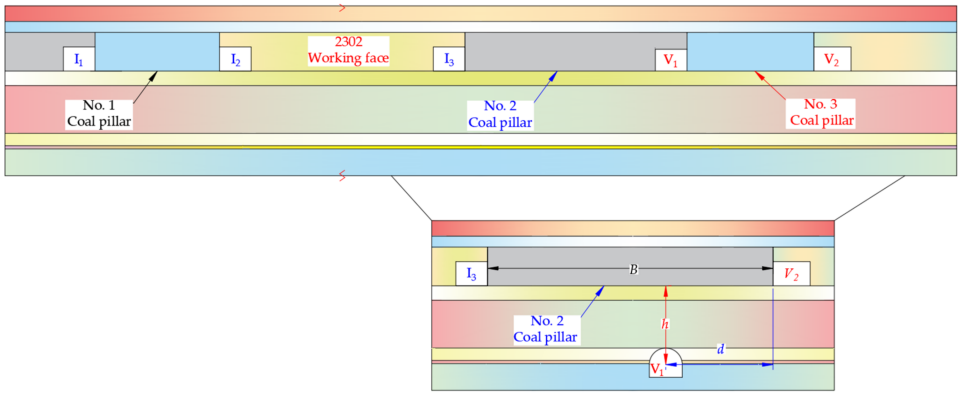

Figure 3. Optimized roadway layout.

V_1 was arranged in floor rock strata after optimization. Meanwhile, reducing the coal pillar size directly on the two working faces could greatly improve the recovery rate of coal resources. V_1 could be excavated in the floor rock strata of coal seams due to low gas content in rock strata. A gas discharge hole was set up aslope in the roadway during the quick excavation of V_1, I_3, and V_2 after gases were discharged. V_1 was excavated in floor strata to ensure its stability. Concentrated floor stress was released to eliminate the heaving floor of V_2.

When the coal pillar size retained between the two working surfaces was too large, it caused resource waste after the roadway layout was optimized. However, when the coal pillar size was too small, the W2302 working face interfered with V_1 and V_2, and the stability of the two return airways was not easy to control. When the vertical distance d between V_1 and the coal seam floor was too small, floor stress was more concentrated, and the stability of surrounding rocks was not easy to control. When d was too large, the

excavation among V_1, I_3, and V_2 was large. To this end, it was necessary to determine the reasonable coal pillar size and the vertical distance between V_1 and the coal seam as well as formulate corresponding technical measures for surrounding rock control.

3. Modeling and Analysis of Reasonable Coal Pillar Sizes

The average coal seam inclination angle in the west wing mining area of Sihe Coal Mine is 4°, and the coal seam is near-horizontal. The coal seam in the mechanical model could be regarded as a horizontal one to facilitate the establishment, analysis, and calculation of the mechanical model. The influences of inclination angles on the coal pillar size were not considered in the calculation process [40,41]. Figure 4 shows the mechanical model established based on the theoretical analysis of the limit equilibrium method.

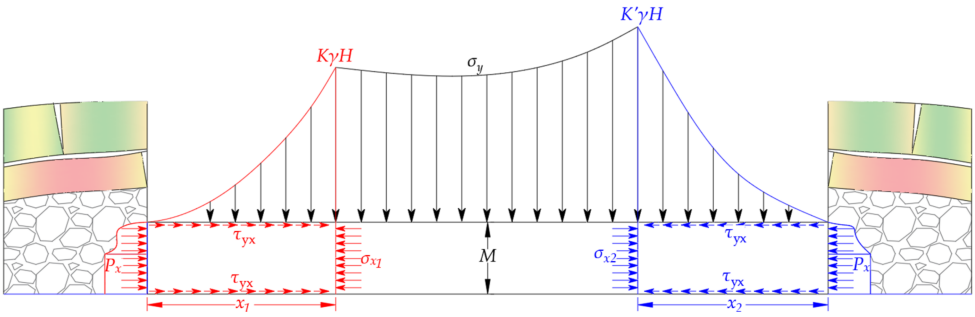

Figure 4. Calculation model of plastic failure areas.

The left side is I_3 of the W1302 working surface, and the right side is V_2 in the mechanical model. The protective coal pillar size should be greater than the sum of the plastic deformation failure area on both sides of the coal pillar and two times the coal pillar height, namely,

$$B \geq x_1 + 2M + x_2 \tag{1}$$

where x_1 and x_2 are the roadway-side coal pillar plastic failure area widths of I_3 and V_2 in the W2302 working face, respectively (m), and M is the coal pillar height (m).

When the side of I_3 is taken as the research object, the plastic failure deformation area and the junction surface of the roof and floor meet the limit equilibrium conditions.

$$\tau_{yx} = -(\sigma_y \tan\varphi_0 + C_0) \tag{2}$$

where τ_{yx} is shear stress on the plastic deformation zone (MPa); σ_y is the vertical stress on the plastic deformation zone (MPa); φ_0 is the internal friction angle at the junction of the coal seam, roof, and floor (°); and C_0 is the cohesive force at the junction of the coal seam, roof, and floor (MPa).

The differential equation can be listed according to the mechanical model.

$$\begin{cases} \frac{\partial \sigma_x}{\partial x} + \frac{\partial \tau_{yx}}{\partial y} = 0 \\ \frac{\partial \tau_{yx}}{\partial x} + \frac{\partial \sigma_y}{\partial y} = 0 \end{cases} \tag{3}$$

The stress boundary condition of the model is

$$\begin{cases} [\sigma_y]_{x=x_1} = K\gamma h \\ [\sigma_x]_{x=x_1} = \lambda [\sigma_y]_{x=x_1} = \lambda K\gamma h \end{cases} \tag{4}$$

where K and K' are the stress concentration coefficients in the coal column, γ is the average unit weight of overlying strata (N/m^3), and h is the average buried depth of the coal seam (m).

Equations (2) and (4) are used to obtain

$$x_1 = \frac{M\lambda}{2\tan\varphi_0} \ln\left[\frac{\lambda K H \tan\varphi_0 + 2C_0}{2(C_0 + P_x \tan\varphi_0)}\right] \tag{5}$$

where λ is the side pressure coefficient and P_x is the side pressure (MPa).

V_2 is used as I_2 of the W2303 working surface. Similarly, the plastic failure deformation area at the V_2 side near the goaf is

$$x_2 = \frac{M\lambda}{2\tan\varphi_0} \ln\left[\frac{\lambda K' H \tan\varphi_0 + 2C_0}{2(C_0 + P_x \tan\varphi_0)}\right] \tag{6}$$

Laboratory tests were carried out through on-site sampling of the working surface of Sihe Coal Mine. The internal friction angle φ_0 of the coal mass is 22.44°, adhesive force C_0 is 2.12 MPa, coal seam thickness M is 6.08 m, and lateral force P_x is 0.1 MPa. The lateral pressure decreases after the roadway is excavated. The side pressure coefficient λ is 0.5, and K and K' are stress concentration coefficients in the coal pillar. The on-site measurements were carried out on the side of the coal pillar of the W2301 working surface to obtain the internal lateral stress concentration coefficients of the coal pillar. A total of 29 drilling stress gauges were set up in the coal pillar (see Figures 5 and 6).

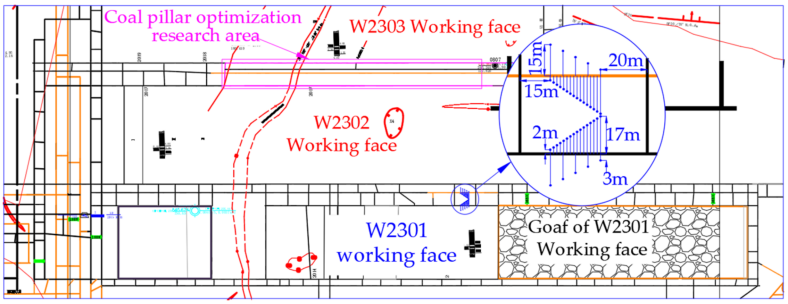

Figure 5. Site measured locations.

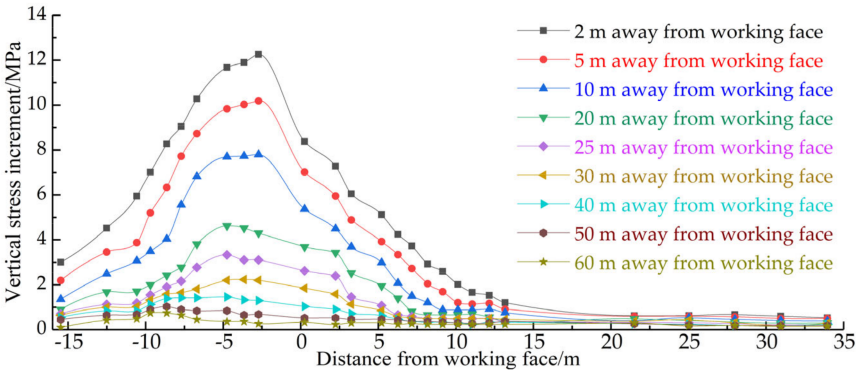

Figure 6. Measured lateral support pressure distribution.

As the distance between the working surface and the station decreased, the support pressure in the coal pillar gradually increased. The lateral support pressure increased first and then decreased from the coal pillar edge on the working surface to the coal pillar inside. The peak distance of the support stress increment is about 14.5 m from the roadway side, the maximum stress increment is 12.2 MPa, the initial injection stress of drilling stress is about 5 MPa, and stress concentration coefficient K is 3.44. When the W2303 work surface is mined, the adjacent W2302 work surface has been mined. The lateral stress value should be greater than the W2302 working surface, and K' should be 1.1 K. Based on the above

values, the x_1 value is 13.30 m, and the x_2 value is 13.60 m. Therefore, the coal pillar width should be greater than 39.06 m.

The coal pillar size of the large-scale and high-comprehensive mining working surface after the roadway layout is optimized should be greater than 39.06 m, according to modeling analysis, laboratory tests, and actual measurement results, while the coal pillar size of the original plan is 55 m. Therefore, the coal pillar sizes of the new scheme can be set to 40, 45, 50, and 55 m.

The plastic failure and deformations of coal rock masses in the mining field under different coal pillar sizes should be studied through finite difference numerical simulation software to seek the optimal roadway layout.

4. Simulation Analysis of the Optimized Roadway Layout

According to the geological profile of the W2302 working face of Sihe Coal Mine, a numerical simulation model with a length of 500 m, a width of 341.9 m, and a height of 57.5 m was established using finite difference numerical simulation software FLAC3D version 6.0. Stress was applied to the top of the model to simulate the unit weight of overlying strata and constrain the surrounding and bottom boundaries. A boundary coal pillar of 50 m was retained on each side of the model to eliminate the influence of the boundary effect. Figure 7 shows the simulation model, and Table 1 shows the parameters of rock strata.

The mechanical parameters of rock strata were assigned after modeling. The working surface was first excavated to derive the lateral support pressure of the working surface after the model reached equilibrium again. The step-by-step excavation of the working surface consistent with the site was performed—each mining roadway was first excavated. The bolt support system of the roadways was established in advance through Rhino software, and then DXF format files were exported. The files were called when the roadway was excavated, and the bolt parameters were given. The W2302 working surface was excavated after the roadway excavation. The main simulation contents referred to the plastic failure of the W2302 mining roadway and the V_1 deformations. Figure 8 shows the lateral stress and roof stress distribution curves.

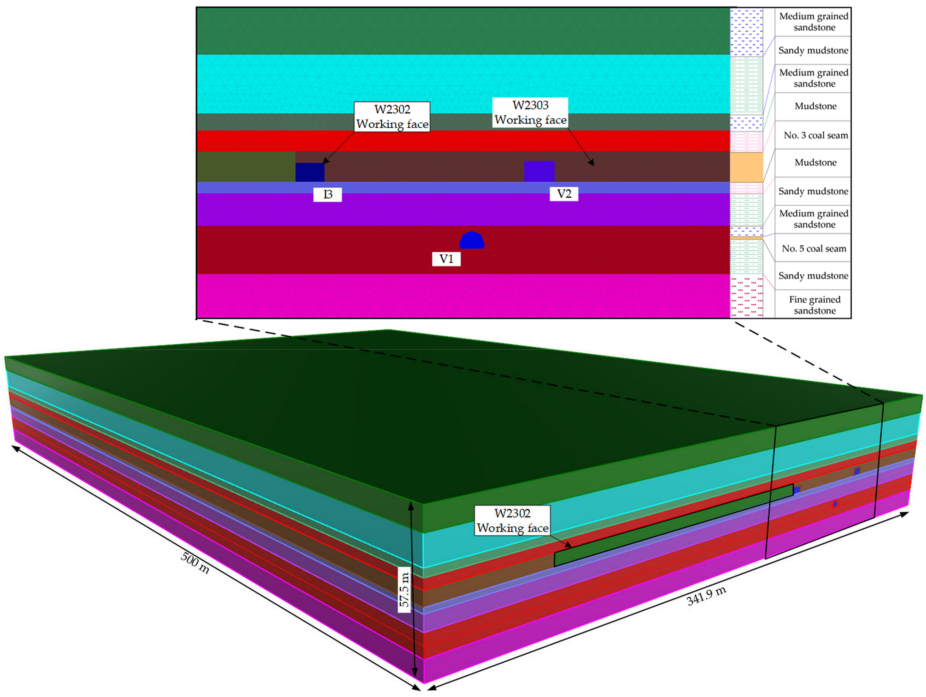

Figure 7. Numerical simulation model.

Table 1. Mechanics parameters of rocks.

Lithology	H (m)	D (kg·m^{-3})	CS (MPa)	B (GPa)	TS (MPa)	C (MPa)	F (°)
Medium grained sandstone	376.85	2602	48.42	29.26	6.56	7.54	33.26
Sandy mudstone	388.65	2576	10.74	23.18	1.68	2.37	23.44
Medium grained sandstone	392.05	2628	46.70	31.40	6.81	7.78	34.26
Mudstone	396.21	2546	16.64	18.90	2.72	2.78	27.62
Coal seam 3$^{\#}$	402.29	1457	6.21	9.77	0.57	2.12	22.44
Mudstone	404.57	2531	16.31	17.32	2.57	2.82	27.36
Sandy mudstone	412.08	2536	11.89	25.18	1.59	2.46	23.58
Medium grained sandstone	414.03	2621	50.36	31.67	2.86	9.74	38.12
Coal seam 5$^{\#}$	414.53	1483	5.89	8.42	0.49	2.03	22.06
Sandy mudstone	420.43	2533	24.51	29.48	1.73	2.57	27.69
Fine-grained sandstone	424.43	2591	38.32	27.57	5.81	6.53	31.22

Note: *H*: buried depth of rock strata; *D*: density; *CS*: compressive strength; *B*: bulk modulus; *TS*: tensile strength; *C*: cohesion; *F*: friction.

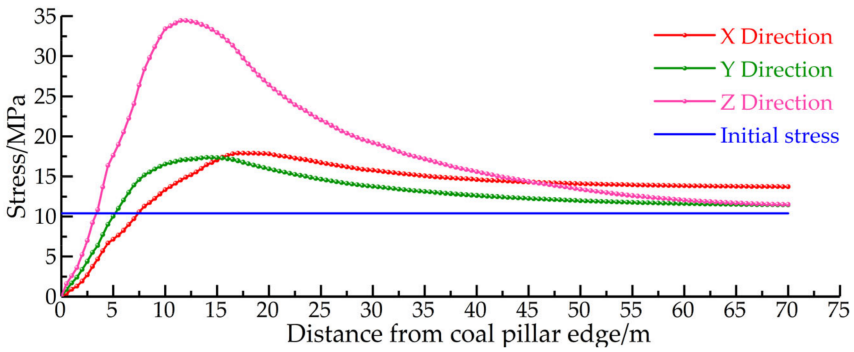

Figure 8. Lateral stress distribution.

Stress changes in the *X* and *Y* axes were small after the working surface was mined, while changes in the *Z* axis (vertical stress) were large (see Figure 8). The initial vertical stress of the coal seam on the working surface was 10.4 MPa, and the vertical stress of the peak was 34.32 MPa after excavation. The distance from the coal pillar edge was 12.5 m, while the lateral stress concentration coefficient was 3.3. Lateral stress gradually flattened as the distance from the coal pillar edge increased. Peak stress in the *X* and *Y* axes was about 17 MPa in the numerical simulation; therefore, the value of pressure measurement coefficient λ was reasonable at 0.5. Numerical simulation results were consistent with the theoretical analysis and on-site measured data after the working surface was mined. Horizontal stress and shear stress changed relatively little, so vertical stress was the most important for selecting the stone drift location of the floor. The vertical stress distribution curve of the floor was derived to find the optimal roadway V_1 layout (see Figure 9).

The vertical stress changed greatly at 10–15 m below the coal pillar and in the coal pillar width of 40–55 m (see Figure 9). The vertical stress concentration coefficients of different coal pillar widths were equal with a stress concentration coefficient of about 1 at 10 m below the coal pillar and about 12 m from the center line of the coal pillar. Medium-grained sandstone was at 9.8–11.8 m below the coal pillar floor, which was suitable for the roof of the roadway and the two sides. Sandy mudstone under medium-grained sandstone was suitable for two sides and the floor of the roadways. Based on theoretical analysis and the distribution of rock formations in the mining field, roadway V_1 used medium-grained sandstone as the roof and two sides and sandy mudstone as the floor (see Table 2 for the specific layout).

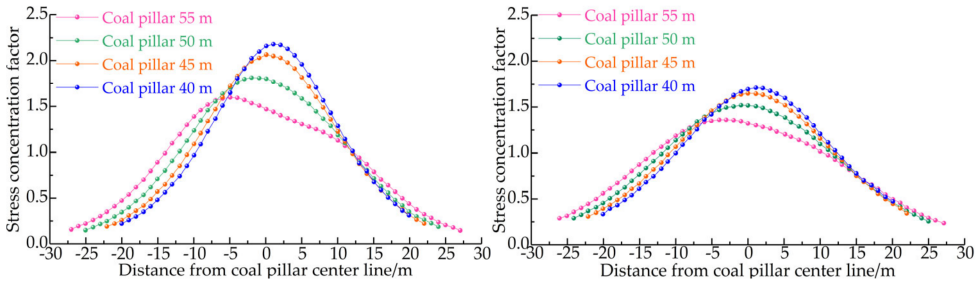

Figure 9. Vertical stress distribution of coal pillar floor: (**a**) 10 m below the coal pillar and (**b**) 15 m below the coal pillar.

Table 2. Optimized roadway layout.

Coal Pillar Width/m	40	45	50	55
Distance from roadway I_3/m	8	10	13	15

According to the optimized position in Table 2, the model was established again to simulate the plastic development of the mining field in different roadway layouts (see Figure 10).

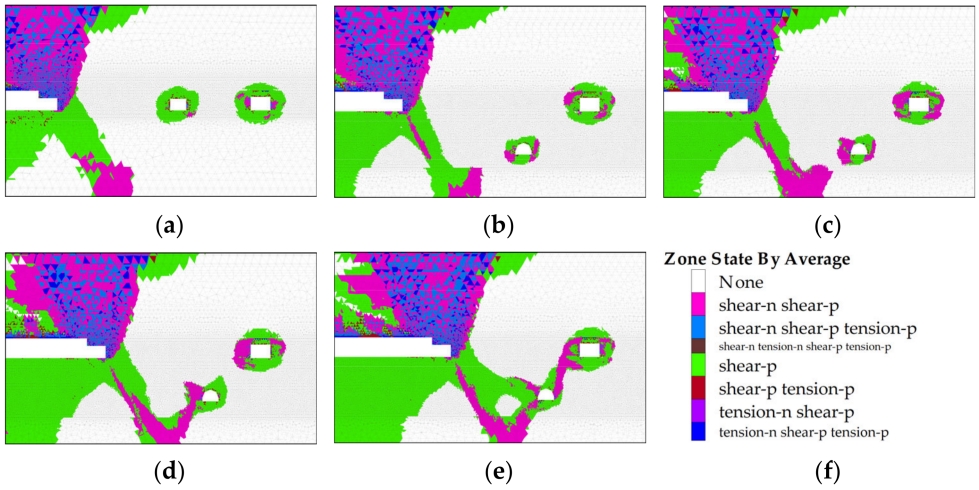

Figure 10. Plastic development of stope affected by actual mining. (**a**) Original plan. (**b**) Coal pillar width of 55 m. (**c**) Coal pillar width of 50 m. (**d**) Coal pillar width of 45 m. (**e**) Coal pillar width of 40 m. (**f**) Legend.

The plasticity of surrounding rocks of V_1 and V_2 was affected by lateral stress, and the weight was increased under the original scheme after the W2302 working surface was mined (see Figure 10). However, the surrounding rocks were relatively stable, the plastic failure area was not connected, and the plastic failure at the base angle of the working surface was serious. When the coal pillar size was 55 m, the two wind lanes were unaffected by actual mining after the roadway layout was optimized. The plastic failure area of V_1 increased after being affected by mining when the coal pillar size was reduced to 50 m, while V_2 was not affected by actual mining. When the coal pillar width was reduced to 45 m, V_1 was greatly affected by mining the W2302 working surface. The plastic failure area of the base angle developed upward after reaching the bottom boundary and was connected with V_1. The plastic failure of V_2 also increased, but the overall change was not large.

As the coal pillar size continued to shrink to 40 m, the plastic development area of the working surface base angle was directly connected to V_1 after the W2302 working

surface was mined. V_1 and V_2 were greatly affected by actual mining, and the plastic development of the two mining roadways was also connected. The surrounding rocks of roadways were difficult to control in this case. The deformation cloud map of V_1 was derived (see Figure 11) to further study the V_1 deformations of the mining roadway on the working surface.

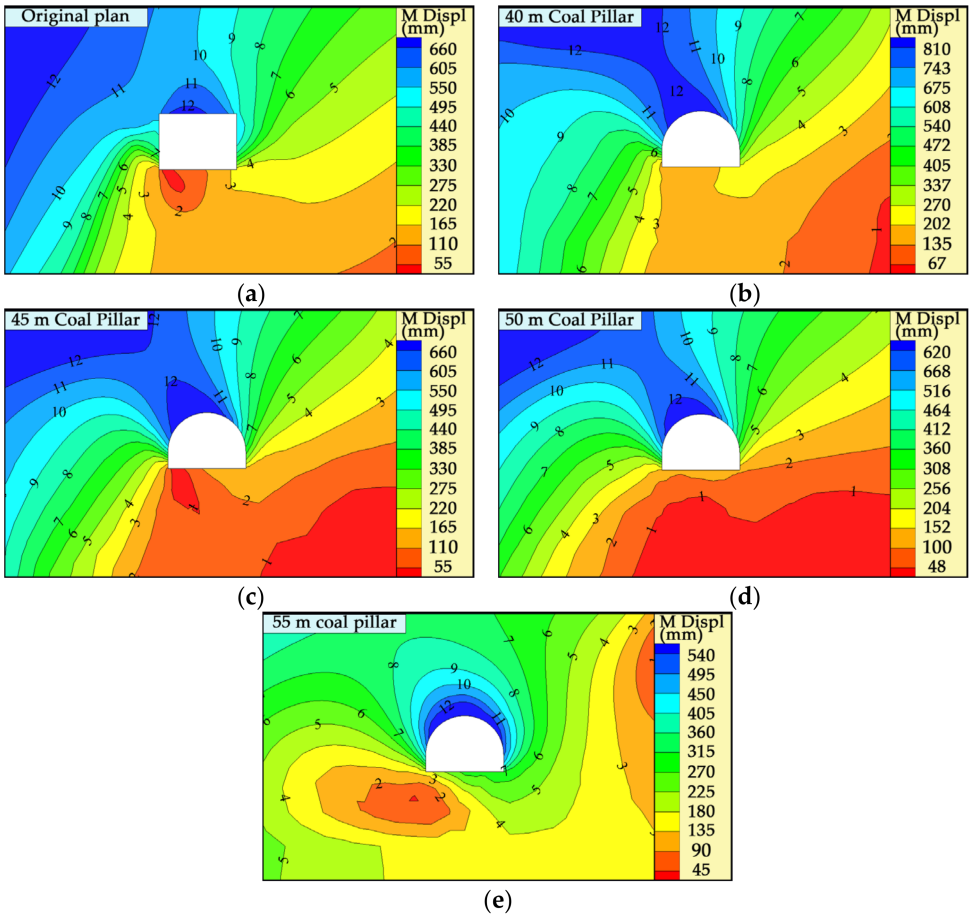

Figure 11. Deformations of surrounding rocks affected by actual mining. (**a**) Original plan. (**b**) Coal pillar width of 40 m. (**c**) Coal pillar width of 45 m. (**d**) Coal pillar width of 50 m. (**e**) Coal pillar width of 55 m.

When the original scheme was adopted, the maximum sinking capacity of the V_1 roof was 660 mm after the W2302 working surface was mined, with the maximum floor heaving capacity of 165 mm and the deformation of the two roadway sides of 400 mm (see Figure 11). When the coal pillar size was 40 m after optimizing the roadway layout, the V_1 deformations were significantly increased compared with the original plan, and the stability of the surrounding rocks of roadways during the service period was not easy to guarantee. When the coal pillar size was increased to 45 m, the V_1 deformations were significantly reduced. The movement of the roadway roof and floor was similar to the original plan, and the two sides were smaller than the original plan. When the coal pillar size increased to 50 m, the deformations of surrounding rocks of V_1 decreased again. However, compared with the coal pillar size of 45 m, the change was not large. When the coal pillar size was 55 m, V_1 showed uniform deformation, which was less affected by the W2302 working surface.

Based on the above plastic development and surrounding rock deformation simulation analysis, the optimized coal pillar size is 45 m. Taking into account the large cross-section size of the W2302 working surface mining roadway and the long service period, it is

necessary to formulate corresponding surrounding rock control technologies for optimized roadways to ensure the stability of surrounding rocks during their service period.

5. Control Technology of Surrounding Rocks after the Optimized Plan

The staggered-layer arrangement of roadways was finally determined through theoretical and numerical analysis combined with the specific engineering practice of the west wing mining area of Sihe Coal Mine. The coal pillar size was 45 m after the optimized plan. However, the plastic development of surrounding rocks was still more serious in this case after return-air stone drift was affected by actual mining, and the deformation amount was still large. Corresponding surrounding rock stability control technology needed to be adopted to ensure the safe and stable use of roadways during the service period. It could directly serve the next working surface in the case of no maintenance or simple maintenance. The technical measures of pressure relief blasting of I_3 and strengthening V_1 support were proposed based on the above requirements and the roadway layout. I_3 was an air inlet roadway, and gas content was small, so the blasting project was progressing more safely. Meanwhile, concentrated floor stress was released after blasting, which reduced the plastic development area. Support for V_1 was strengthened to ensure the safe and stable use of V_1 during the service period.

A comparative test of similar simulations was used to explore the influences of pressure relief blasting on the stability of surrounding rocks of roadways because the finite difference numerical simulation software could not achieve the blasting effect. The roadway on the left side of the model was not loosened and blasted under the original support, while the right side was loosened and blasted under the support scheme (see Figure 12). A fuse was used as the bolt, and gypsum cement was used as the anchoring agent in the simulation process. A WY30-VIIIA high-precision hydraulic regulator was used as the loading control device to apply the load, and the vibrating soil pressure gauge was used to monitor the roadway floor stress during the test. Broken rock masses were removed by crushing and blasting to enhance the blasting effect during the simulation process.

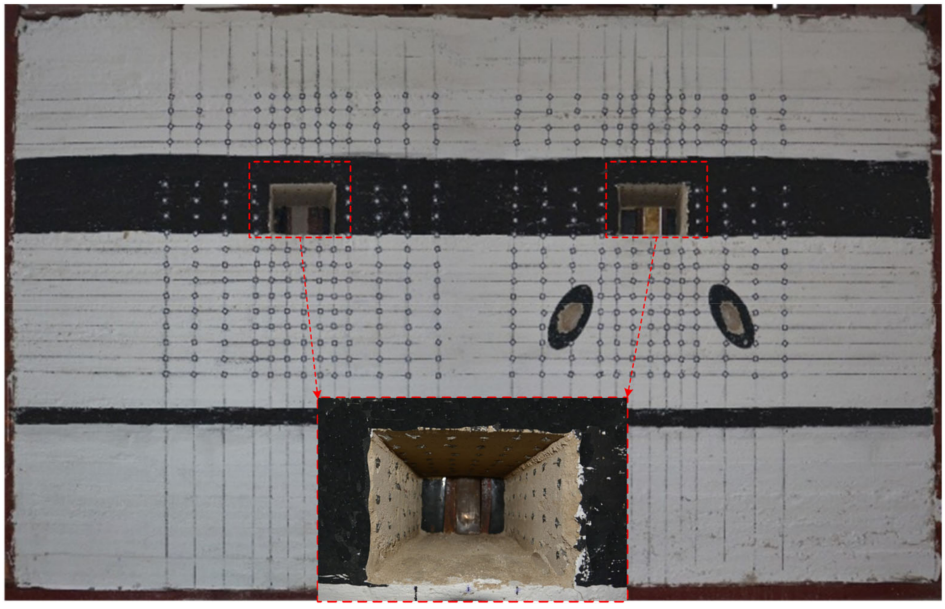

Figure 12. Similar simulation model.

Heaving floor occurred in both pressure relief blasting and non-blasting (see Figures 13 and 14). However, unexploded roadways were severely damaged, and the roof was broken. The wall caving of the two sides was serious, and the maximum movement between the two sides was 20 mm. The heaving floor of blasted roadways was small, and the roof was relatively complete. The deformations of the two sides were slower, and

the two sides moved closer by about 10 mm. Floor deformations were even more different in the two cases. Heaving floor before the pressure relief blasting of roadways was 20 mm; that after pressure relief was 14 mm and reduced by 43%, and the pressure relief effect was obvious. The amount of deformation of the surrounding rocks of un-loosened blasting roadways was relatively continuous, and that of the loosened blasting roadway decreased sharply near the pressure relief blasting zone (20 to 30 cm below roadways). The pressure relief blasting zone absorbed part of the deformations and controlled the floor deformations. Deformations were more obvious in the area at 45 cm below the roadway floor when it was not exploded. However, the rock masses in this area were not changed after pressure relief blasting. The stress of the roadway floor is shown in Figure 15.

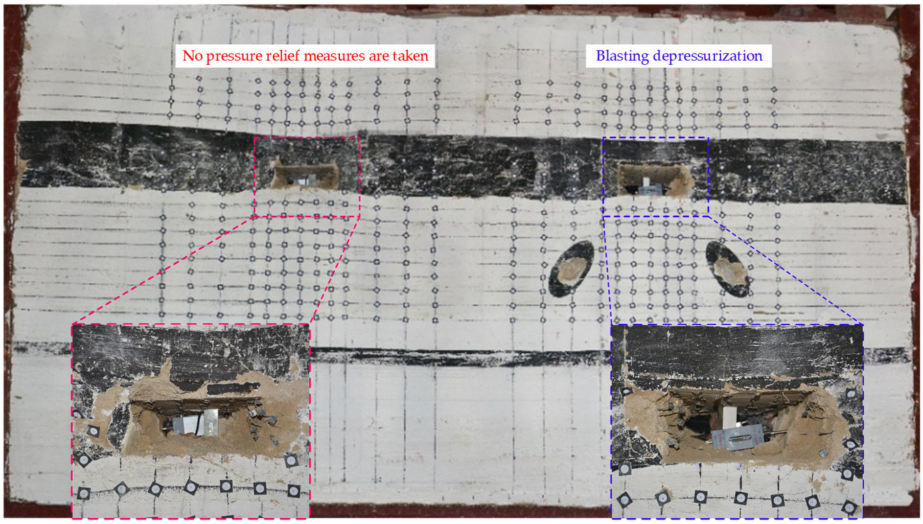

Figure 13. Comparison of unexploded and blasting effects.

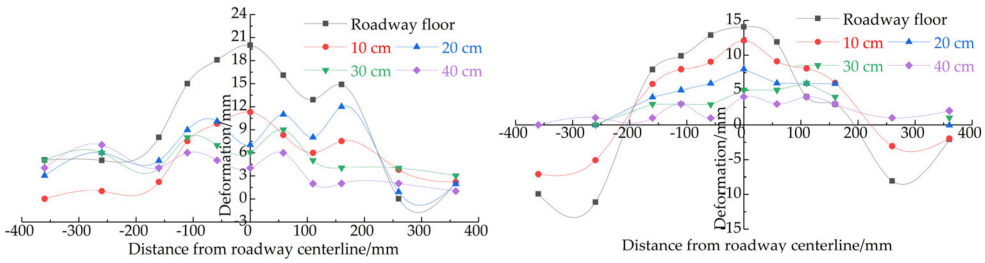

Figure 14. Deformation of similarly simulated roadway floor. (**a**) Deformation of unexploded floor. (**b**) Deformation of blasting floor.

When 0.7 MPa was loaded, the floor stress value in the 120 and 480 mm areas under the roadway floor without pressure relief blasting was about 0.39 MPa in a similar simulation test. However, the stress concentration in the 240 mm area under the roadway floor was higher, and the stress concentration value was 0.212 MPa. Stress on the rock strata in the 120 and 240 mm areas under the floor after pressure relief blasting was 0.049 and 0.056 MPa, respectively. Stress on the rock masses in the 480 mm area below the floor was 0.212 MPa.

Horizontal concentrated stress in the shallow surrounding rocks and concentrated stress in the original stress concentration area were transferred to the deep rock strata after pressure relief blasting. The shallow rock strata and the roadway surface were released. According to similar simulation test results, the floor stress could be released, and floor deformation could be controlled. The stability of the surrounding rocks of I_3 could be controlled after pressure relief blasting. Stress concentration in the area where V_1 was located has also been released, and the environment of the surrounding rocks of V_1 has

been improved. V_1 and V_2 served two working surfaces, and the service period was longer. Little or no maintenance was required during the service period of the two working faces to ensure the stability of the surrounding rocks in the service period of V_1 and V_2. Support technology for V_1 and V_2 was enhanced (see Figure 16).

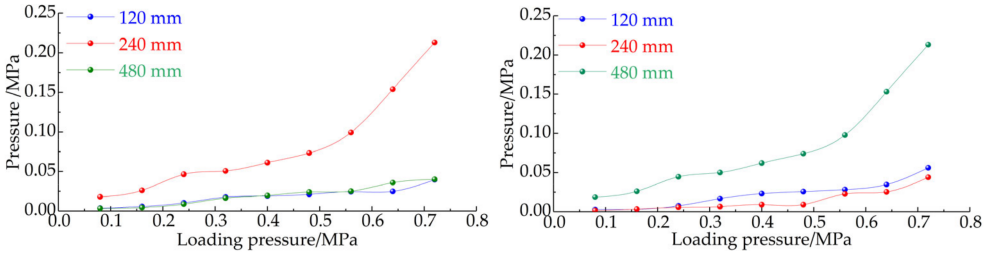

Figure 15. Stress on similarly simulated roadway floor. (**a**) Stress on unexploded floor. (**b**) Stress on blasted floor.

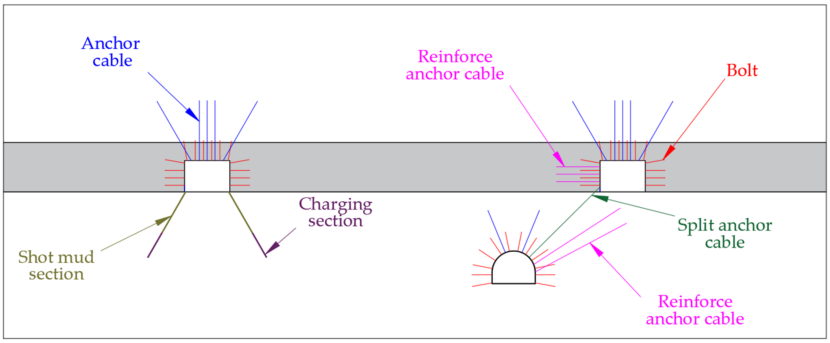

Figure 16. On-site implementation plan.

The pressure relief blasting of base angles was implemented in I_3 (see Figure 16). The inclination angle of the pressure relief hole was 30°, and the length was 9.2 m. The length of the charge section was 3.4 m, and that of the stemming blocking section was 5.8 m. Mutual-pulling bolts between V_1 and V_2 were established. V_1 was provided with a reinforced bolt toward V_2, and V_2 was provided with a reinforced bolt toward the coal pillar.

6. On-Site Deformation Monitoring of Surrounding Rocks

Surface displacement monitoring stations are arranged in V_1 and V_2 to test the optimization of the roadway layouts and the reliability of the surrounding rock control technology. The V_1 monitoring station is 100 m away from the working surface, and Figure 17a shows the deformations of the surrounding rocks during excavations. The distance of the V_2 measuring station from the working surface was 21 m, and Figure 17b shows the displacement and deformations of the working surface during excavations.

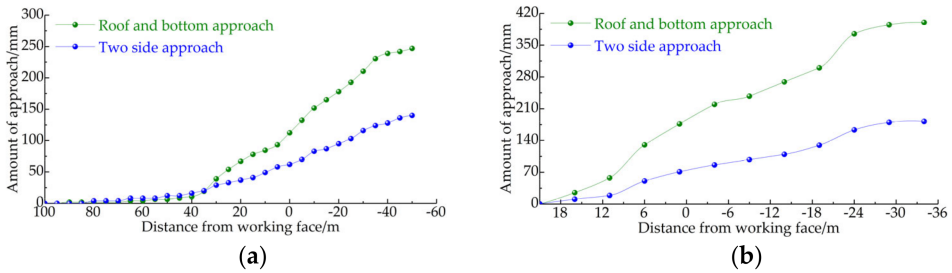

Figure 17. Deformation monitoring of surrounding rocks. (**a**) Deformation monitoring of roadway V_1. (**b**) Deformation monitoring of roadway V_2.

Roadway deformations were not obvious before the station was 40 m away from the working surface (see Figure 16). As the distance between the station and the working surface decreased, the deformation rate of roadways increased significantly. When the working surface was pushed over the station for about 40 m, V_1 entered a stable state. The maximum movement of roof and floor was 260 mm, and that of the two sides was 147 mm. V_2 was excavated along the coal seam floor, and coal masses were at the roof. The deformation amount during the excavation of the working surface was larger than that of V_1, but the horizontal distance between the roadway and the W2302 working surface was larger.

When the working surface was pushed about 30 m after the station, the movement deformations of surrounding rocks of the roadway reached a stable state, and the maximum movement of the roof and floor was about 410 mm. The maximum movement of the two sides was 142 mm because the roadway side was equipped with reinforced bolts. The deformation monitoring results of surrounding rocks of the on-site roadway showed that two return airways were less affected by actual mining. They could be simply repaired and directly serve the next working surface without repair. Mine pressure monitoring results showed that pressure relief blasting and strengthening support technology proposed by this work could control the deformations of surrounding rocks and ensure the safe and stable use of roadways during the service period.

7. Discussion of Research Results

The minimum coal pillar retained size was determined through modeling and analysis of the stress of coal pillars in the west wing mining area of Sihe Coal Mine. The reasonable retained size of coal pillars and the specific locations of the staggered-layer arrangement of roadways were determined by numerical simulation software combined with the specific rock strata distribution on the site. The technical measures of pressure relief blasting and strengthening support were proposed, and the feasibility of the plan was verified through similar simulation tests.

However, the geological conditions targeted by this work are relatively simple, and the optimization of roadway layout and the surrounding rock control technology under inclined coal seams and special geological conditions are not involved. The optimization of the coal pillar and the surrounding rock control technology of high-gas mines under inclined coal seams and special geological conditions will be studied at a later stage. It will ensure safe and efficient production under different mining conditions and maximize the recovery rate of coal resources.

8. Conclusions

This work used the high-gas content, large-scale mining, and high-comprehensive mining working surface of the west wing mining area of Sihe Coal Mine as the background in Shanxi, China. The roadway layout was optimized through theoretical analysis, numerical simulation, and other methods, and the corresponding surrounding rock control technology was proposed.

1. A mechanical model of the load-bearing failure of the coal pillar was established, and parameters affecting the coal pillar width were determined through laboratory tests and on-site measurements. The minimum coal pillar retained size was 39.06 m, which improved the recovery rate of coal resources and ensured the gas treatment effect of the working surface.
2. An optimization plan for the staggered-layer layout of the mining roadway was proposed based on the gas treatment conditions of the high-gas working surface. The optimized roadway layout and the reasonable coal pillar size were determined through numerical simulations. The technical measures of pressure relief blasting and strengthening support were proposed for the optimized roadway.
3. The feasibility of blasting pressure relief technology was verified through a similar simulation test, and the I_3 roadway was successfully applied. The reinforcing anchor

cable was installed to strengthen the support in the area with severe plastic damage in the simulation. The field application effect was good, which can provide reference for similar projects.

Author Contributions: Conceptualization, Q.M. and Y.Z. (Yidong Zhang); methodology, L.H.; software, Z.L. and Y.Z. (Yu Zheng); validation, G.S.; formal analysis, Q.M.; writing—original draft preparation, Q.M.; writing—review and editing, Y.Z. (Yidong Zhang) and Q.M.; project administration, Y.Z. (Yu Zheng). All authors have read and agreed to the published version of the manuscript.

Funding: This work was funded by the Key Project of Joint Funds of the National Natural Science Foundation of China (Grant No. U1903209).

Institutional Review Board Statement: Not applicable.

Informed Consent Statement: Not applicable.

Acknowledgments: The authors would like to thank the engineering technicians in Shaping Coal Mine for their enthusiastic assistance and suggestions.

Conflicts of Interest: The authors declare no conflict of interest.

References

1. Zhang, T. Discussion on the Current Situation and Development Trend of Energy Utilization in China. *Territ. Nat. Resour. Study* **2021**, *5*, 76–78.
2. Zheng, C.; Zhang, Y.; Long, L. Study on National Principal Energy Consumption Structural Modulation and Optimization in New Era. *Col. Geo. Chi.* **2021**, *33*, 49–51.
3. Hou, C.J. *Roadway Surrounding Rock Control*; China University of Mining and Technology Press: Xuzhou, China, 2013.
4. Zhang, H.; Wang, D.X.; Wang, Q.F. Analysis on Characteristics of Major and Above Coal Mine Accidents in China from 2005 to 2016. *J. Saf. Environ.* **2019**, *19*, 1847–1852.
5. Zhang, J.W.; Yang, C.X. Statistical Analysis of Major and Above Coal Mine Accidents in China from 2005 to 2019 and Research on Safety Production Countermeasures. *Saf. Coal Mines* **2021**, *52*, 261–264.
6. Ma, Q.; Zhang, Y.D.; Li, Z.X. The Roadway Layout and Control Technology of Pillar-Free Mining of Soft Coal Seams in High Gassy Mines. *Processes* **2022**, *10*, 1784. [CrossRef]
7. Ma, Q.; Zhang, Y.D.; Gao, L.S. The Optimization of Coal Pillars on Return Air Sides and the Reasonable Horizon Layout of Roadway Groups in Highly Gassy Mines. *Sustainability* **2022**, *14*, 9417. [CrossRef]
8. Meng, H. Optimization Analysis of Roadway Layout in Close Coal Seam Based on Energy Release Method. *Saf. Coal Mines* **2018**, *49*, 194–198.
9. Xu, H.J. *Research on Optimized Layout and Support Technology of Roadways in Extremely Close Coal Seam Mining*; China University of Mining and Technology: Xuzhou, China, 2016.
10. Meng, H. Research on Optimization of Roadway Layout in Lower Coal Seam of Close Coal Seam Group. *Coal Sci. Technol.* **2016**, *44*, 44–50.
11. Zhang, C.L.; Zhang, Y. Study on Optimization of Roadway Layout for Simultaneous Mining of Close Seams. *Coal Sci. Technol.* **2014**, *42*, 53–56.
12. Zhao, Y.H.; Song, X.M.; Liu, N.B. Study on Pillar Stability and Roadway Layout Optimization in Shallow Seam Group. *Coal Sci. Technol.* **2015**, *43*, 12–17.
13. Li, H.C.; Bai, J.B. Study on Optimization of Coal Pillar Roadway Layout under the Influence of Mining. *Saf. Coal Mines* **2019**, *50*, 166–172.
14. Wang, G.L.; Chang, Y.B.; Ling, L. Research on Roadway Layout Optimization and Combined Support Technology in Three Soft Coal Seam. *Coal Eng.* **2022**, *54*, 55–61.
15. Mohammad, Z.; Irfan, A.S. Numerical Analysis of Himalayan Rock Tunnels under Static and Blast Loading. *Geotech. Geol. Eng.* **2021**, *39*, 5063–5083.
16. Sun, B.X. Optimization and Application of Roadway Layout in Fully Mechanized Top Coal Caving Face of Baode Coal Mine. *Coal Eng.* **2021**, *53*, 7–12.
17. Zaid, M.; Rehan Sadique, M. A Simple Approximate Simulation Using Coupled Eulerian– Lagrangian (CEL) Simula-tion in Investigating Effects of Internal Blast in Rock Tunnel. *Indian Geotech. J.* **2021**, *51*, 1038–1055. [CrossRef]
18. Mohammad, Z.; Swapnil, M. Numerical Analysis of Shallow Tunnels Under Static Loading: A Finite Element Approach. *Geotech. Geol. Eng.* **2021**, *39*, 2581–2607.
19. Kang, H.P. 60 Years and Prospect of Bolting Technology Development in Coal Mine Roadway in China. *J. China Univ. Min. Technol.* **2016**, *45*, 1071–1081.
20. Kang, H.P.; Jang, P.F.; Feng, Y.J. Coal Mine Roadway Surrounding Rock Pressure Relief Technology and Application. *Coal Sci. Technol.* **2022**, *50*, 1–15.

21. Kang, H.P. Development and Prospect of Surrounding Rock Control Technology in Coal Mine Roadway in China for 70 years. *Chin. J. Rock Mech. Eng.* **2021**, *40*, 1–30.
22. Zhang, Y.D.; Cheng, L.; Yang, J.F. Experimental Study on the Influence of Bolt Support Density on Bearing Characteristics of Anchored Composite Bearing Body. *J. Min. Saf. Eng.* **2015**, *32*, 305–309.
23. Zhang, Y.D. *Study on Bearing Characteristics of Anchored Composite Bearing Body and its Application in Roadway Bolt Support Design*; China University of Mining and Technology: Xuzhou, China, 2013.
24. Ma, Q.; Zhang, Y.; Zhang, X.; Li, Z.; Song, G.; Cheng, J.; Gao, K. The Failure Law and Control Technology of Large-Section Roadways in Gently Inclined Soft Coal Seams. *Processes* **2022**, *10*, 1993. [CrossRef]
25. Gao, L.S.; Deng, G.Z.; Zhang, M.L. Surrounding Rock Control of Soft Rock Roadway Based on Anchored Composite Bearing Body Theory. *Min. Res. Dev.* **2021**, *41*, 140–144.
26. Cheng, J.Y.; Wei, Z.J.; Bai, J.C. Research on Floor Heave Control Technology of Deep Tectonic Stress Water Rich Soft Rock Roadway Based on Blasting Pressure Relief. *Coal Sci. Technol.* **2022**, *50*, 117–126.
27. Li, C.J. *Study on Blasting Pressure Relief Mechanism and Surrounding Rock Stability of Deep Roadway*; Anhui University of Science and Technology: Huainan, China, 2021.
28. Yu, W.J.; Li, K.; Lu, Q.H. Engineering Characteristics and Deformation Control of Surrounding Rock of Roadway in Fractured Rock Mass. *J. China Coal Soc.* **2021**, *46*, 3408–3418.
29. Zuo, J.P.; Shi, Y.; Liu, D.J. Equivalent Elliptical Model and Simulation Analysis of Slotting and Pressure Relief in Deep Soft Rock Roadway. *J. China Univ. Min. Technol.* **2019**, *48*, 1–11.
30. Gu, M.; Jiang, G. Stability Control Technology for Roof Surrounding Rock of Deep Soft Rock Roadway. *Coal Eng.* **2011**, *9*, 29–30.
31. Sadique, M.; Zaid, M.; Alam, M. Rock Tunnel Performance Under Blast Loading Through Finite Element Analysis. *Geotech. Geol. Eng.* **2022**, *40*, 35–56. [CrossRef]
32. Zaid, M.; Sadique, M.; Alam, M. Blast Resistant Analysis of Rock Tunnel Using Abaqus: Effect of Weathering. *Geotech. Geol. Eng.* **2022**, *40*, 809–832. [CrossRef]
33. Zaid, M. Preliminary Study to Understand the Effect of Impact Loading and Rock Weathering in Tunnel Constructed in Quartzite. *Geotech. Geol. Eng.* **2022**, 1–29. [CrossRef]
34. Mishra, S.; Zaid, M.; Rao, K.S.; Gupta, N.K. FEA of Urban Rock Tunnels Under Impact Loading at Targeted Velocity. *Geotech. Geol. Eng.* **2022**, *40*, 1693–1711. [CrossRef]
35. Zaid, M. Dynamic Stability Analysis of Rock Tunnels Subjected to Impact Loading with Varying UCS. *Geo. Eng.* **2021**, *24*, 505–518.
36. Zaid, M. Three-dimensional finite element analysis of urban rock tunnel under static loading condition: Effect of the rock weathering. *Geo. Eng.* **2021**, *25*, 99–109.
37. Zhi, R.W. Study on Surrounding Rock Control Technology of Gob Side Entry with Large Mining and Large Section. *Coal Eng.* **2022**, *54*, 27–33.
38. Zhu, C.; Yuan, Y.; Wang, W.M. Research on the "Three Shells" Cooperative Support Technology of Large-section Chambers in Deep Mines. *Int. J. Min. Sci. Technol.* **2021**, *31*, 665–680. [CrossRef]
39. Yang, J.H.; Jiang, Z.S.; Xie, S.R. Stability Analysis and Control Technology of Surrounding Rock at Intersection of Deep Large Section Roadway. *Coal Sci. Technol.* **2020**, *48*, 49–56.
40. Su, C.; Lu, J.; Guo, Y. Determination of Reasonable Size of Coal Pillar in High Gas Fully Mechanized Top Coal Caving Face Section. *Min. Saf. Environ. Prot.* **2018**, *45*, 89–92.
41. Qian, M.G.; Shi, P.W.; Xu, J.L. *Ground Pressure and Strata Control*; China University of Mining and Technology Press: Xuzhou, China, 2010.